Higher Order Boundary Elements: A Facilitating Technique for Advancing the Modelling of the Forward Oscillating Vessel Interaction Analysis

Grant E. Hearn*

Hydromechanics Research Group,
Marine Technology Department,
University of Newcastle upon Tyne,
NEI 7RU, U.K.

ABSTRACT

The higher order boundary element (HOBE) method is discussed in the context of a new formulation of the forward speed problem. In particular, after reviewing the different forward speed formulations considered in the literature a formulation which includes the interaction of the steady and unsteady wave systems is proposed. Since the proposed formulation assumes solution is possible using a Green Function Matching (GFM) technique this method is investigated in the context of the zero speed problem. The hemisphere and barge examples presented will indicate the type and level of the different numerical problems to be overcome if the HOBE based GFM technique is to be successfully applied to the proposed forward speed formulation.

INTRODUCTION

The forward speed fluid-structure interaction analysis is required to analyse structures steadily advancing in an incident wave system, and to provide improved predictions of the behaviour of moored structures in a random seaway [1]. For fine-form ship structures the forward speed may be included implicitly using different strip-theory based methods [1,2,3]. However, for moored ships the generalised strip-theory of reference [1] was found to be inadequate for predicting the second order quantities of added resistance and surge low frequency damping. For barges and other offshore floating structures a general 3D method is necessary [4]. Therefore in this paper it is implicit throughout that 3D rather than 2D formulations are being discussed.

The motivation for the research reported stems from the recognised need to improve the prediction of the second-order forces and moments experienced by moored floating structures [1,4]. Improvements in the hydrodynamic modelling leads to distinctly different estimates of the horizontal excursions of moored structures in a random seaway [5]. In this respect the influence of choice regarding the selection of combinations of first-order interaction analysis solvers and second-order force and moment predictors is another important issue [6,7]. Thus the improvements sought are not driven by a need to improve first-order solvers per se, but to improve second-order analyses which are dependent upon the quality of the first-order solvers used.

A thorough review of the formulation of the forward-speed fluid-structure interaction has recently been presented by the author [8]. In particular, the wetted surface and free-surface boundary conditions were discussed in the light of including the interaction between the steady and unsteady motions experienced by an advancing body. If this interaction is neglected then the more common forward speed analysis formulation [9] is retrieved. In this case direct application of Green's second identity provides a number of different fluid-structure interaction formulations in terms of velocity potential or source strength [10]. The Green function associated with each of the alternative Fredholm integral equation based formulations is dependent upon:

- implicit or explicit inclusion of forward speed effects
- automatic satisfaction, or otherwise, of free-surface, seabed and radiation boundary conditions.

Similarly the size and extent of the solution domain is dependent upon the extent to which the selected Green function satisfies the latter cited group of conditions.

Solution of the Fredholm integral equations has generally been solved, within the Newcastle hydromechanics research group, using boundary element techniques. Both open water and confined water (in-tank) applications are solvable using either the Sommerfeld radiation condition or a far-field eigenfunction expansion solution matching condition on the radiation surface [11]. The explicit inclusion of forward speed effects introduces waterline contour integrals in the velocity potential and source strength formulations. Hence more sophisticated numerical solvers are required if the free-surface contour contributions are to be

* Senior Lecturer and Head of Hydromechanics Research Group.

determined on the actual free-surface. To this end a HOBE based Green function method and a HOBE Green function matching technique have been developed.

HOBE techniques employ the use of curved boundary elements with a higher order functional representation of the unknown quantity over the boundary element. Here, 'serendipity elements', in the terminology of finite elements [12], are used. In such elements the approximations used only depend upon the support of 'nodes' on the boundary of the element. The interpolation functions or shape functions used are simple polynomials in terms of the local curvilinear coordinates over each element. Such ideas were introduced by Hess nearly twenty years ago [13,14,15] for analysing both non-lifting and lifting 2D aerofoil sections. Hearn & Donati [16] extended the application of HOBE methods to 2D free-surface fluid-structure interaction analyses. In developing seakeeping applications Hearn & Donati found Hess' conclusion, that the order of the shape functions describing the higher order boundary element geometry,and the unknown behaviour of the fluid over the elements, must be one degree different, unnecessary. Hearn & Lau [17] then extended the ideas of Hearn & Donati [18] to 3D fluid-structure interaction analyses using a non-interacting steady-unsteady formulation.

In the remainder of this paper we shall discuss the modified forward speed problem and its possible solution using a HOBE based GFM technique. Numerical problems associated with this technique will be highlighted by solving simpler problems.

FORWARD SPEED MODELLING

Assuming no interaction between the steady (wave-making resistance) potential Φ_s and the 'unsteady' (seakeeping) potential Φ_u, the standard formulation of the first-order forward speed problem is

$$\begin{aligned} \nabla^2\Phi_u &= 0 \text{ everywhere in the fluid,} \\ \left[g\frac{\partial}{\partial z}+\left(\frac{\partial}{\partial t}-U\frac{\partial}{\partial x}\right)^2\right]\Phi_u &= 0 \text{ on } S_f, \text{ the free-surface,} \\ \frac{\partial}{\partial n}\left[\phi^I+\phi^S\right] &= 0 \text{ on } S_w, \\ \frac{\partial}{\partial n}\phi^k &= -i\omega_e n_k + U m_k \text{ on } S_w, \end{aligned} \tag{1}$$

upon assuming that

$$\Phi_u = \left[\phi^I+\phi^S+\Sigma_{k=1}^{6}\eta_k\phi^k\right]exp(-i\omega_e t), \tag{2}$$

and the encounter wave frequency, ω_e, and the incident wave frequency, w, satisfy

$$w_e = w - \frac{2\pi}{\lambda}U\cos\beta. \tag{3}$$

The terms n_k and m_k associated with the wetted-surface radiation boundary conditions for the radiation potentials, ϕ^k, are dependent on the description of the normal velocity of the wetted-surface, S_w. Setting $U = 0$ obviously provides the corresponding zero speed formulation.

To include the steady and unsteady wave interaction the dynamic free-surface condition is derived by applying Bernoulli's equation in the form

$$\eta = -\frac{1}{g}\left[\frac{D}{Dt}\Phi+\frac{1}{2}|\nabla\Phi|^2\right], \tag{4}$$

with the Lorentz operator,

$$\frac{D}{Dt} = \frac{\partial}{\partial t}+\nabla\Phi_s\cdot\nabla. \tag{5}$$

Using these equations and neglecting higher order terms of $\nabla\Phi_s$ the new proposed free-surface boundary condition may be written [19] as

$$\left[g\frac{\partial}{\partial z}+\left(\frac{\partial}{\partial t}-U\frac{\partial}{\partial x}\right)^2\right]\Phi_u+2\left(\frac{\partial}{\partial t}-U\frac{\partial}{\partial x}\right)(\nabla\Phi_s\cdot\nabla\Phi_u) = 0 \text{ on } S_f. \tag{6}$$

The first compound term of this free-surface condition is similar to the non-interacting free-surface boundary condition of Equation (1). However, Equation (6) differs from the composite free-surface condition of Grue & Palm [20], and Zhao & Faltinsen [21], as they used a corrected non-linear Bernoulli equation and a linearised kinematic free-surface condition to generate the corresponding composite free-surface boundary condition.

To determine the wetted-surface boundary conditions two distinct reference systems are considered, namely the inertial (space-fixed) reference system $Oxyz$ and the body-fixed reference system $O'x'y'z'$ considered to be coincident with the inertial reference system when the structure is at rest. The origin O is located in the undisturbed free-surface, $z = 0$. If the position of O' with respect to O is $\underline{\xi} = (\xi_1,\xi_2,\xi_3)$, then the position vectors of a generic point satisfy

$$\underline{X}' = D(\underline{X}-\underline{\xi}), \tag{7}$$

with

$$\underline{X} = (x,y,z) \text{ or } (x_1,x_2,x_3), \tag{8}$$

$$\underline{X}' = (x',y',z') \text{ or } (x_1',x_2',x_3'), \tag{9}$$

and D represents a rotational transformation. If the rotation is finite and the order of rotation is roll, pitch and yaw, say, with respective amplitudes ξ_4, ξ_5 and ξ_6, then $D = C\,B\,A$, with A, B and C satisfying

$$A = \begin{pmatrix} 1 & 0 & 0 \\ 0 & cos\xi_4 & sin\xi_4 \\ 0 & -sin\xi_4 & cos\xi_4 \end{pmatrix} \tag{10}$$

$$B = \begin{pmatrix} cos\xi_5 & 0 & -sin\xi_5 \\ 0 & 1 & 0 \\ sin\xi_5 & 0 & cos\xi_5 \end{pmatrix} \tag{11}$$

and

$$C = \begin{pmatrix} cos\xi_6 & sin\xi_6 & 0 \\ -sin\xi_6 & cos\xi_6 & 0 \\ 0 & 0 & 1 \end{pmatrix}. \tag{12}$$

The order of the rotation operators A, B and C must be preserved.

By expanding the sine and cosine functions higher-order representations of the vessel displacement due to rotations may be derived. In particular, we may write,

$$\underline{X} = \underline{X}' + [\underline{\xi} + \underline{\alpha} \wedge \underline{X}'] + \epsilon^2 H \underline{X}' + O(\epsilon^3) \quad (13)$$

where $\underline{\alpha} = (\xi_4, \xi_5, \xi_6)$,

$$\epsilon^2 H = -\frac{1}{2} \begin{pmatrix} (\xi_5^2 + \xi_6^2) & 0 & 0 \\ -2\xi_4\xi_5 & (\xi_4^2 + \xi_6^2) & 0 \\ -2\xi_4\xi_6 & -2\xi_5\xi_6 & (\xi_4^2 + \xi_5^2) \end{pmatrix}, \quad (14)$$

and the term $O(\epsilon^3)$ indicates that cubic and higher order terms and products have been neglected.

If $\underline{V}_s$ and $\underline{V}$ denote the velocity of the structure and the fluid velocity respectively, then continuity of velocity across the instantaneous wetted surface S' requires

$$\left(U\underline{i} + \dot{\underline{d}} - \nabla\Phi\right) \cdot \underline{n} = 0, \quad (15)$$

where U is the speed of the vessel, $\underline{i}$ is the unit vector associated with the forward speed, $\underline{d} = \underline{\xi} + \underline{\alpha} \wedge \underline{X}'$ is the first-order displacement vector of Equation (13), and

$$\Phi = U\chi_s + \Phi_u. \quad (16)$$

Rearranging, it follows that

$$\left(\dot{\underline{d}} - \nabla\Phi_u - \underline{W}\right) \cdot \underline{n} = 0 \text{ on } S', \quad (17)$$

where $\underline{W} = \nabla\Phi_s = U\ \nabla(\chi - x)$ and x is the direction of the structure's uniform translation, as measured with respect to S_m, the wetted-surface described with respect to $Oxyz$. Since

$$\underline{W} \cdot \underline{n} = 0 \text{ on } S_m \quad (18)$$

only when the vessel is purely translating, then

$$\frac{\partial\Phi_u}{\partial n} = \dot{\underline{d}} \cdot \underline{n} - \underline{W} \cdot \underline{n} \text{ on } S'. \quad (19)$$

The equivalent boundary condition applicable on S_m is determined following Newman [22]. Taking into account the rotation and gradient effects upon $\underline{W}$ the equivalent first-order representation becomes

$$\frac{\partial\Phi_u}{\partial n} = \left[\dot{\underline{d}} + \nabla\wedge\left(\underline{\alpha} \wedge \underline{W}\right)\right] \cdot \underline{n} \text{ on } S_m, \quad (20)$$

upon appealing to Equation (18). This form of the boundary condition was originally derived by Timman & Newman [23] to account, in a consistent manner, for the interaction between the steady and oscillatory flow fields. In many earlier ship-motion analyses an incomplete form of Equation (20) was used and this led to an erroneous asymmetry between the coupling of heave and pitch.

Reduction of Equation(20) to appropriate scalar radiation wetted-surface boundary conditions leads to

$$\frac{\partial}{\partial n}\phi^k = -i\omega_e n_k + m_k'. \quad (21)$$

The outward normal $\underline{n}$ and the generalised direction cosine are given respectively by

$$\underline{n} = (n_1, n_2, n_3), \quad (22)$$

$$\underline{n} \equiv \underline{X}' \wedge \underline{n} = (n_4, n_5, n_6), \quad (23)$$

and the forward speed related terms m_k' satisfy

$$\underline{m}' \equiv -(\underline{n} \cdot \nabla)\underline{W} = (m_1', m_2', m_3') \quad (24)$$

and

$$\underline{m}' \equiv -(\underline{n} \cdot \nabla)(\underline{X}' \wedge \underline{W}) = (m_4', m_5', m_6'). \quad (25)$$

These wetted-surface conditions now include the interaction between the steady and unsteady waves. A discussion of the singular nature of the m_k' terms for 2D flows solved using low order boundary elements has been presented by Zhao & Faltinsen [24].

If χ, the wavemaking velocity potential, is now ignored, then $\underline{W} \equiv -U\underline{i}$, and $m_k' : k = 1,2,3,4$ becomes zero and m_5' and m_6' satisfy the well known expressions

$$m_5' = +Un_3 \text{ and } m_6' = -Un_2. \quad (26)$$

Comparison of Equation (1) with Equations (21) to (25) implies that $m_k' = Um_k$ when the steady-unsteady interactions are neglected.

BOUNDARY ELEMENT FORMULATIONS

The general boundary is assumed to consist of the wetted-surface S_w, the radiation or control surface S_r, the free-surface S_f and the sea-bed S_b. Since the formulations now presented are primarily for deep water, the seabed impermeability condition and the behaviour of the Green function G will usually remove S_b from the integral equation formulations generated.

Zero Speed Formulation

Assuming the velocity potential is to be determined directly then the choice of second kind Fredholm integral equations to be considered is

$$-\alpha\phi + \int_{S_w} \phi\frac{\partial G}{\partial n}ds = \int_{S_w} G\ v_n ds, \quad (27)$$

when G satisfies all the required boundary conditions except the wetted-surface boundary condition, on which $v_n = \frac{\partial\phi}{\partial n}$, and

$$\begin{aligned} -\alpha\phi + \int_{S_w} \phi\frac{\partial G}{\partial n}ds + \int_{S_r}\left[\phi\frac{\partial G}{\partial n} - G\frac{\partial\phi}{\partial n}\right]ds \\ + \int_{S_f}\left[\phi\frac{\partial G}{\partial n} - \frac{\omega^2}{g}\phi G\right]ds = \int_{S_w} G\ v_n ds \end{aligned}, \quad (28)$$

when the simpler Rankine source Green function, $G = \frac{1}{r}$, is selected. Here r is the distance between the fluid singularity point and some generic point in the fluid. The term $\frac{\partial\phi}{\partial n}$ on S_r in Equation (28) is now modelled using either the Sommerfeld radiation condition expressed in the form

$$\frac{\partial\phi}{\partial n} \equiv \frac{\partial\phi}{\partial r} = \left[i\nu - \frac{1}{2r}\right]\phi, \quad (29)$$

or, specified using some other matching technique. Here ν is the wavenumber.

The equivalent source strength formulation corresponding to Equation (27) is

$$-\alpha\sigma = \int_{S_w} \sigma \frac{\partial G}{\partial n} ds - v_n \,, \tag{30}$$

with

$$\phi = \int_{S_w} \sigma G ds. \tag{31}$$

Standard Forward Speed Formulation

The corresponding translating and pulsating source based Green function integral equations for ϕ and σ are respectively

$$\begin{aligned} -\alpha\phi + \int_{S_w} \phi \frac{\partial G}{\partial n} ds - 2i\frac{U\omega_e}{g} \oint_{L_0} G\phi dy \\ + \frac{U^2}{g} \oint_{L_0} [\phi \frac{\partial G}{\partial x} - G\frac{\partial \phi}{\partial x}] \, dy = \int_{S_w} G \, v_n ds \end{aligned} \,, \tag{32}$$

and

$$-\alpha\sigma = \int_{S_w} \sigma \frac{\partial G}{\partial n} ds + \frac{U^2}{g} \oint_{L_0} n_1 \sigma \frac{\partial G}{\partial n} dy - v_n \,, \tag{33}$$

with ϕ recoverable from

$$\phi = \int_{S_w} \sigma G ds \,. \tag{34}$$

The contour L_0 is the undisturbed free-surface waterline. In this formulation the Timman-Newman [23] reverse flow symmetry relationship for G has been used to reduce the free-surface contribution to the equivalent waterline contour integral.

Unsteady-Steady Interacting Forward Speed Formulation

The generality of the free-surface and wetted-surface boundary conditions expressed in Equations (6) and (21)-(25) respectively do not readily lead to a convenient all embracing Green function. Therefore the solution domain is split into an inner and outer region. In the inner region the proposed governing equation is

$$\begin{aligned} -\alpha\phi + \int_{S_w} \phi \frac{\partial G}{\partial n} ds + \int_{S_r} [\phi \frac{\partial G}{\partial n} - G\frac{\partial \phi}{\partial n}] ds \\ + \int_{S_f} [\phi \frac{\partial G}{\partial n} - \frac{\partial \phi}{\partial n} G] ds = \int_{S_w} G \, v_n ds \end{aligned} \,, \tag{35}$$

and G is assumed to be the Rankine source Green function. Here the control surface, S_r, is an 'open box' consisting of some vertical arbitrary shaped cylindrical wall and a flat bottom. External to the 'box' control surface the fluid is infinite in extent (both radially and with depth). It is now assumed that the non-linear nature of the unsteady-steady interaction is less dominant as the observer moves further and further from the wetted surface of the structure, S_w. Thus in the outer region we may consider the flow as being modelled by the standard forward speed integral equation of Equation (32) with S_w and L_o now corresponding to the 'box' control surface and its intersection with the free-surface. Across the 'box' control surface the inner and outer solutions must be matched to provide continuity of ϕ and normal velocity. Since $\frac{\partial \phi}{\partial n}$ is not known a ' priori on the 'box' control surface then the indicated modified form of Equation (32) must be used to provide the required normal derivative on the box. Thus the Fredholm equation is now treated as first kind, whereas when using it to determine ϕ it is second kind. This is possible, see below, because G is known (under the assumptions made) in the outer problem and continuity of ϕ across the control surface is a natural boundary condition on S_r. This approach has been designated the Green function matching (GFM) approach.

Clearly, prior to solving this more complex problem it is prudent to investigate whether the simpler standard zero speed and standard forward speed problems can be satisfactorily solved using the HOBE GFM technique.

Green Function Matching Technique Formulations

Matching inner and outer solutions is not an uncommon procedure [11]. Often in offshore engineering analysis an inner finite element solution is matched to an outer boundary element solution to reduce the finite element solution domain and to provide automatic satisfaction of the far-field radiation boundary condition. Here, letting S_r denote the described 'box' control surface, we now reformulate the zero speed and standard forward speed problems in the context of the proposed GFM technique. In all the presented inner problem formulations the Rankine source form of Green function is to be used.

Zero Speed Formulation

Here the inner problem formulation is exactly the same as the alternative zero speed formulation of Equation (28), viz

$$\begin{aligned} -\alpha\phi + \int_{S_w} \phi \frac{\partial G}{\partial n} ds + \int_{S_r} [\phi \frac{\partial G}{\partial n} - G\frac{\partial \phi}{\partial n}] ds \\ + \int_{S_f} [\phi \frac{\partial G}{\partial n} - \frac{\omega^2}{g} \phi G] ds = \int_{S_w} G \, v_n ds \end{aligned} \,, \tag{36}$$

but now rather than specify $\frac{\partial \phi}{\partial n}$ on S_r using a Sommerfeld radiation condition, or some other matching condition [11], the required control boundary derivative is now determined using the relationship

$$\left[\frac{\partial \phi'}{\partial n}\right] = [G]^{-1} \left[\frac{\partial G}{\partial n}\right] [\phi'] \tag{37}$$

which is generated by treating the Fredholm integral equation

$$-\alpha\phi' + \int_{S_r} \phi' \frac{\partial G}{\partial n} ds = \int_{S_r} G \frac{\partial \phi'}{\partial n} ds. \tag{38}$$

as a first-kind integral equation for the required derivative.The negative sign correctly accounts for the difference in the sign of the outward normal on S_r for the inner and outer problems and ϕ' is the outer solution.

Standard Forward Speed Formulation

The inner Rankine source based formulation is now a generalisation of Equation (36), viz

$$-\alpha\phi + \int_{S_w} \phi \frac{\partial G}{\partial n} ds + \int_{S_r} \left[\phi \frac{\partial G}{\partial n} - G \frac{\partial \phi}{\partial n}\right] ds + \int_{S_f} \left[\phi \frac{\partial G}{\partial n} - \frac{1}{g}\left[\omega_e + iU\frac{\partial}{\partial x}\right]^2 \phi G\right] ds = \int_{S_w} G\, v_n ds \quad , \quad (39)$$

whereas the outer integral equation is Equation (32) modified to reflect the new free-surface boundary condition, that is,

$$-\alpha\phi' + \int_{S_r} \phi' \frac{\partial G}{\partial n} ds - 2i\frac{U\omega_e}{g} \oint_{L_r} G\phi' dy + \frac{U^2}{g} \oint_{L_r} \left[\phi' \frac{\partial G}{\partial x} - G\frac{\partial \phi'}{\partial x}\right] dy = \int_{S_r} G \frac{\partial \phi'}{\partial n} ds \quad , \quad (40)$$

where G is now the velocity potential of a pulsating translating source. Equation (40) is treated as a first-kind integral equation in terms of the normal derivative of the velocity potential on the radiation boundary S_r.

Unsteady-Steady Interacting Forward Speed Formulation

The inner formulation requires satisfaction of Equation (6) on the free-surface. Thus direct substitution into Equation (35) yields

$$-\alpha\phi + \int_{S_w} \phi \frac{\partial G}{\partial n} ds + \int_{S_r} \left[\phi \frac{\partial G}{\partial n} - G \frac{\partial \phi}{\partial n}\right] ds + \int_{S_f} \left[\phi \frac{\partial G}{\partial n} - \frac{1}{g}\left[\left[\frac{\partial}{\partial t} - U\frac{\partial}{\partial n}\right]^2 \phi + \left[\frac{\partial}{\partial t} - U\frac{\partial}{\partial n}\right](\nabla\phi_s \cdot \nabla\phi)\right] G\right] ds = \int_{S_w} G\, v_n ds \quad , \quad (41)$$

and the outer integral equation formulation (under the stated assumptions) is the same as Equation (40) with the same pulsating translating source Green function.

HOBEs AND THE GFM TECHNIQUE

In a number of the Green function based formulations presented the solutions are generated using flat panels and the assumption that the sought unknown velocity potential or source strength is invariant over the individual panels. However, given the complexity of the free-surface boundary conditions, in particular the occurrence of first and second order derivatives of the unknown velocity potential in the above GFM formulations, the use of HOBEs provides an obvious way of processing such terms using the associated shape functions and their derivatives [10,17]. Within the developed zero speed and standard forward speed HOBE Green function and HOBE GFM codes both quadratic and cubic representations of the unknown function over quadrilateral and triangular elements are provided. The number of nodes per element are therefore 8 and 6, and 12 and 10 for the quadratic and cubic representations respectively. For plane boundary elements one node is located at the element centroid.

In Equation (41) the derivatives of the steady wave-making potential ϕ_s are required to formulate the wetted-surface boundary conditions. If the wave-making resistance formulation is linearised then the governing integral equation for a Green function formulation will be analogous to the zero speed seakeeping formulation with the wavenumber $k = \omega^2/g$ being replaced by g/U^2. Hence appropriate modification of the zero HOBE analysis can be used to provide ϕ_s and its derivatives. Thereafter the HOBE GFM approach is used as indicated.

Completeness of the proposed formulations requires explicit definitions of the outer domain associated zero speed pulsating and forward speed translating pulsating Green functions. These may be found in many references and therefore details are not provided here.

TESTING HOBE GFM TECHNIQUES

To assess new procedures some baseline solutions are required. Here, we shall examine the HOBE GFM technique by comparing predictions with

- the MATTHEW 3D Diffraction Analysis Suite,
- the HOBE Green Function Solver.

The MATTHEW 3D diffraction analysis, developed by the author, has been thoroughly tested within industry (UK and overseas) analysing realistic offshore situations. Also many undergraduate and research students at Newcastle University and other Universities have used the MATTHEW suite.

The direct HOBE Green function analysis has been used in different industrial collaborative research programmes [17,25]. The HOBE GFM computer code can also be invoked in a Sommerfeld radiation condition matching mode using Equation (29).

Comparisons of predictions based on both of these analyses and the HOBE GFM predictions are made for a heaving and surging hemisphere. Next the HOBE Green function and HOBE GFM predictions of the hydrodynamic reactive coefficients for an offshore barge, previously studied in reference [4] as Barge C, are compared.

Satisfactory comparisons of low order and high order boundary element predictions of added resistance and drift forces for the Pinkster semi-submersible and Pinkster barge were reported earlier [10]. In this study only first order quantities are reported for the indicated geometries. In presenting any subset of a large number of calculations undertaken, it is easy to select results which place a numerical procedure in a particularly good or bad light, depending upon the conclusion preferred. In the limited space available I will endeavour to avoid this dilemma by presenting only those results which demonstrate a particular potential numerical problem. I shall therefore deliberately omit the more readily acceptable results.

PRESENTATION OF RESULTS

In the calculations undertaken one plane of geometric symmetry has been exploited in the HOBE calculations and two geometric planes of symmetry were exploited in the MATTHEW predictions.

The Hemisphere Predictions

Figures 1 and 2 present discretisations of the inner zero speed formulation for a hemisphere of radius 10m. The first discretisation, designated C, was considered the natural discretisation by a colleague, whereas the second discretisation, F, was considered the more natural discretisation according to the author. This clearly demonstrates the point that the discretisation process is very subjective. Other cruder discretisations of the hemisphere which reflect the personal preferences of C & F were designated A & B and D & E respectively. These applications are not discussed in any detail. However, one can note that only discretisation C has a third band of free surface (inner formulation) boundary elements.

For discretisation F the differences between the HOBE Green function, the Sommerfeld matching, the HOBE GFM and the MATTHEW results are negligibly small for the heave reactive coefficients. However, either an ill conditioned formulation or an irregular frequency occurs near 1.6 rad./sec. for the HOBE Green Function predictions. For discretisation C the HOBE Green function and HOBE GFM heave predictions are sandwiched between the MATTHEW (highest) and SOMMERFELD (lowest) results, which differ by 8% to 10%. If the Sommerfeld matching results are rejected (a reasonable response) this spread in the results drops to about 2% with the MATTHEW and the HOBE GFM results very close. The location of the 'focal point' in the hemisphere discretisation radically affects the performance of the Sommerfeld matching technique, and yet the C and F discretisations of the actual hemisphere are simple rotations of identical representations. Since the MATTHEW predictions are invariant it appears that the HOBE Green Function analysis is a little more sensitive to the discretisation process.

The surge added mass predictions show common trends, with the SOMMERFELD & GFM predictions and the MATTHEW & HOBE Green function predictions naturally pairing in a distinct matter at the higher frequencies, see Figures 3 and 4. The corresponding surge fluid damping coefficients again exhibit ill conditioned formulations or irregular frequencies for the Sommerfled & HOBE GFM predictions presented in Figures 5 and 6. The second peaks in Figures 5 and 6 would be very much narrower were more points included in the plots. In presenting the results a general curve fitting routine rather than straight line linking of the actual predictions was used. This tends to generate non-physical artificially exaggerated sweeps in the plots.

The Barge Predictions

Five discretisations, A to E, were used to represent the box control surface. The discretisation of the wetted-surface of the barge remained invariant whereas the location of the flat bottom of the control surface was gradually lowered. In Figure 7 discretisation E is presented. Figures 8 and 9 present the heave added mass predictions for HOBE calculations based on the Sommerfeld matching and the GFM techniques respectively. As the distance between the (1/100th scale) barge and the flat bottom of the control surface is increased from 3m to 8m so the HOBE Green function and Green function matching technique converge towards one another. If the number of elements on the cylindrical wall of the control surface are doubled when the bottom control surface is 8m from the free-surface (results designated Sommerfeld and Matching in Figures 8 & 9) there is negligible improvement in the predictions. Thus it is the location of the flat bottom which is causing the numerical problem and not the number of elements used to represent the cylindrical control surface. For large barge structures we may conclude that if the flat bottom of the control surface is too near the structure spurious solutions are generated by both forms of the HOBE Green function matching technique.

Further improvements require increasing the distance between the sides of the barge and the vertical sides of the box control surface. These observations also apply to the corresponding surge fluid damping predictions of Figures 10 and 11.

FINAL COMMENTS AND CONCLUSIONS

The Green function matching technique has been proposed as a possible solution method for analysing the proposed formulation of the steady-unsteady interacting forward speed problem. The differences between this formulation, the standard forward speed formulation and the zero speed formulation can be readily identified from Equations (41), (39) & (36) respectively. The success or failure of the technique therefore rests with being able to adequately include the increasing complexity of the free-surface boundary conditions and the generation of an appropriate outer solution or matching technique. In an earlier papers and reports [10,17,18] sufficient mathematical details were provided to demonstrate how the first and second order derivatives of the free-surface boundary conditions could be dealt with using HOBE techniques. These details can be carried across to the new proposed formulation.

In Reference [10] HOBE Green function second order force predictions were generated which were comparable with other researchers low order boundary element predictions and experimental measurements. In this paper the Sommerfeld matching technique has been shown to be a poor predictor of first order results. This appears to contradict earlier published low order boundary element Sommerfeld matching applications [11], although proximity of the control surface has always be a diffi-

cult factor to overcome when using Sommerfeld matching. Some thought is required to explain the increased sensitivity of this problem as a result of using HOBEs.

It would appear that the break down of the Sommerfeld matching procedure is also an indicator of the failure of the HOBE GFM technique. Where numerical resonance occurs in the Sommerfeld results it would appear that the HOBE GFM method is likely to exhibit the same trend. However, whereas the Sommerfeld matching procedure certainly is not suitable for solving the forward speed problem the HOBE GFM has been used successfully.

When analysing a semi-submersible, in earlier work [10], we concluded that location of the matching control surface wasn't too important. For barges this conclusion has clearly been refuted and this is most likely explained by the geometric differences. The free-surface effects are much stronger over the bottom of the barge than over the legs of a semi-submersible.

The boundary element representation of the structure is important in the GFM procedure, as the presented hemisphere results show. In fact, whereas the MATTHEW and HOBE Green function predictions were generally in agreement and insensitive to the different discretisations, the HOBE GFM predictions oscillated between the two and could be made to match either by modifying the discretisations. Whereas in the direct Green function methods (HOBE and LOBE) irregular frequencies, as a cause of numerical resonances, are well understood it is not so simple to explain the numerical resonances in the GFM technique. It could be due to the implied operator of Equation (37), required to provide the normal velocity on the control surface, becoming ill-conditioned. The research must continue. Whereas it is quite clear that overcoming the mathematical difficulties of modelling the free-surface conditions can be achieved using HOBEs, the numerical problems resulting from the coupling of Fredholm integral equations of first and second kind requires further mathematical investigation and numerical studies.

ACKNOWLEDGEMENTS

Thomas Kwok is thanked for undertaking the detailed calculations reported. Helen Clough is thanked for word processing the paper. The research reported was funded by the Science and Engineering Research Council Marine Technology Directorate and the UK Ministry of Defence. Opinions expressed remain the responsibility of the author.

REFERENCES

1. Salvesen, N., Tuck, E.O. and Faltinsen, O.M., "Ship Motions and Sea Loads", Trans. SNAME, Vol. 20, 1970, 250-287.

2. Hearn, G.E. and Tong, K.C., "Evaluation of Low-Frequency Wave Damping", OTC Paper 5176, Vol. 1, 1986, 229-241.

3. Petersen, J.B. & Marnaes, L., "Comparison of Non-Linear Strip Theory Predictions and Model Experiments", Centre for Applied Mathematics and Mechanics, Technical University of Denmark, Lyngby, Report No. 387, April 1989.

4. Hearn, G.E. and Tong, K.C., "A Comparitive Study of Experimentally Predicted Wave Drift Damping Coefficients", OTC Paper 6136, Vol. , 1989, 699-714.

5. Hearn, G.E., Lau, S.M. and Tong, K.C., "Wave Drift Damping Influences Upon the Time Domain Simulations of Moored Structures", OTC Paper 5632, Vol. , 1988, 155-167.

6. Hearn, G.E., Tong, K.C. and Lau, S.M., "Hydrodynamic Models and Their Influence on Added Resistance Predictions," Proceedings of Practical Design of Ships and Mobile Units (PRADS), Vol. I, 1987, 302-316.

7. Hearn, G.E. and Goodwin, P., "Far-Field and Near-Field Investigations of Second Order Force Predictions", Submitted for Publication.

8. Hearn, G.E., "Seakeeping Theories: Spoilt for Choice?", Trans. NECIES, Vol. 107, No. 2, March 1991, 45-66 & Vol. 107, No. 3, June 1991, 109-112 for Discussion and Author's Reply.

9. Wehausen, J.V and Laitone, E.V., "Surface Waves", Handbuch der Physik, Vol. IX, 446-757.

10. Hearn, G.E., "Higher Order Boundary Elements: An Applicable Concept for Hydrodynamic Analysis?", 19th Scientific and Methodological Seminar on Ship Hydrodynamics, (SMSSH), Vol. 2, Paper, No. 60, 1990, 60.1-60.8.

11. Hearn, G.E. and Liou, S.Y., "Finite Depth and Tank Wall Effects upon First and Second Order Forces", Proceeding of Offshore Mechanics and Arctic Engineering, Vol. 1, Part A, 1990, 171 - 180.

12. Zienkiewicz, O.C., "The Finite Element Method", McGraw Hill, 1977.

13. Hess, J.L., "Higher-Order Numerical Solution of the Integral Equation for the Two-Dimensional Neumann Problem", Computer Methods in Applied Mechanics and Engineering, Vol. 2, 1973, 1-15.

14. Hess, J.L., "Improved Solution for Potential Flow About Arbitrary Axisymmetric Bodies by the Use of a Higher-Order Surface Source Method", Computer Methods in Applied Mechanics and Engineering, Vol. 5, 1975, 297-308.

15. Hess, J.L., "The Use of Higher-Order Surface Singularity Distributions to Obtain Improved Potential Flow Solutions for Two-Dimensional Lifting Airfoils", Computer Methods in Applied Mechanics and Engineering, Vol. 5, 1975, 11-35.

16. Hearn, G.E. and Donati, E., "A New Fluid-Structure Interaction Analysis Based on Higher-Order Boundary Elements", Int. J. Numerical Methods in Fluids, Vol. 8, 1988, 199-225.

17. Hearn, G.E. and Lau, S.M., "Low Frequency Damping Predictions and Behaviour of Marine Structures in a Seaway", SERC MTD Floating Production Systems Managed Programme, 1987-89, Final Contract Report, Dec. 1989.

18. Hearn, G.E. and Donati, E., "Higher Order Boundary Elements", SERC MTD Compliant Systems Cohesive Programme, 1983-1985, Final Contract Report, Nov. 1985.

19. Hearn, G.E. and Kwok, T., "Formulating the 3D Low Forward Speed Problem to Include Steady-Unsteady Interactions", SERC MTD/MoD Progress Report, Newcastle University, Dec. 1990.

20. Grue, J. and Palm, E., "Currents and Wave Forces on Ships and Marine Structures", IUTAM Memorial Symposium to Professor R.E.D. Bishop on the Dynamics of Marine Vehicles and Structures in Waves, Developments in Marine Technology, 7, Edited by W.G. Price, P. Temarel and A.J. Keane, Elsevier, 1991, 167-180.

21. Zhao, R. and Faltinsen, O.M., "Interaction Between Waves and Current on a Two Dimensional Body in the Free Surface", J. Applied Ocean Res., Vol. 10, No. 2, april 1988, 87-99.

22. Newman, J.N., "The Theory of Ship Motions", Advances in Applied Mechanics, Vol. 18, 1978, 221-283.

23. Timman, R. and Newman, J.N., "The Coupled Damping Coefficients of a Symmetric Ship", J. Ship Research, Vol. 5, No. 4, March 1962, 1-7.

24. Zhao, R. and Faltinsen, O.M., "A Discussion of the m_j in the Wave - Body Interaction Problem", Fourth Int. Workshop on Water Waves and Floating Bodies, 1989, 275-279.

25. Floating Production systems in Waves. Results from a comparative study on Hydrodynamic Coefficients, Wave Forces and Motion Responses. FPS 2000, A NTNF Research Programme, Norway 1990.

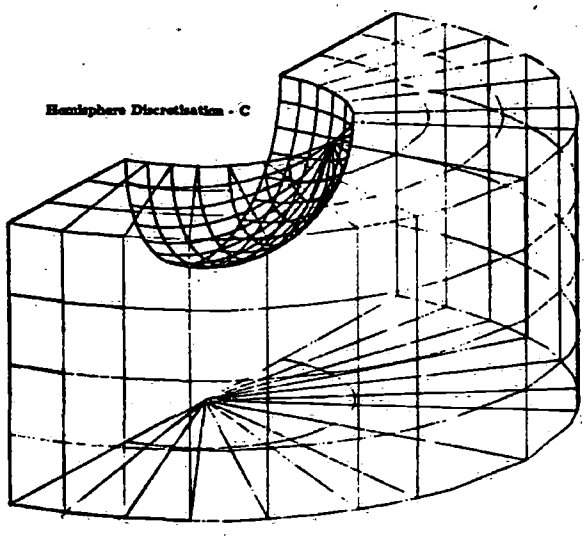

Figure 1. Hemisphere Discretisation C for Inner Formulation.

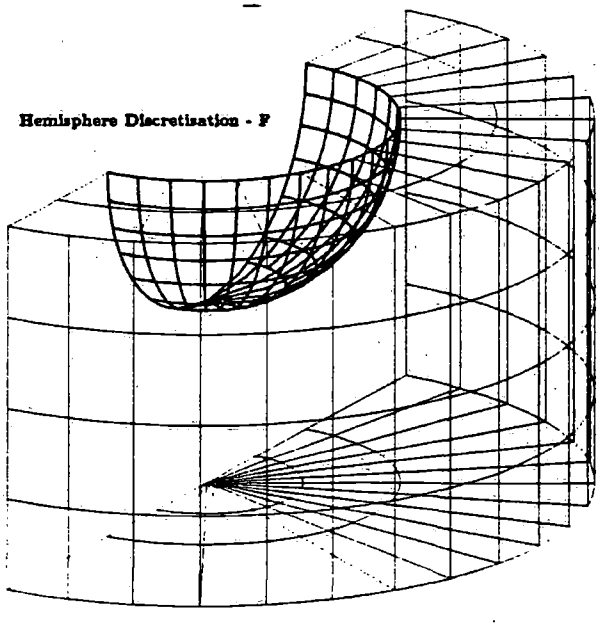

Figure 2. Hemisphere Discretisation F for Inner Formulation.

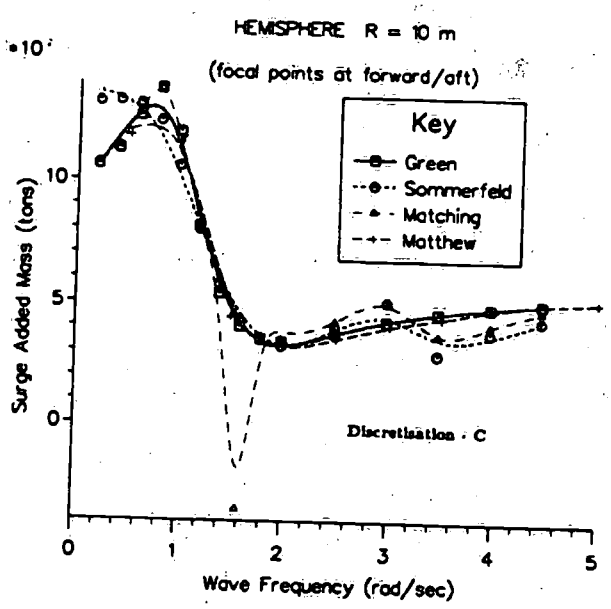

Figure 3. Discretisation C Surge Added Mass Predictions.

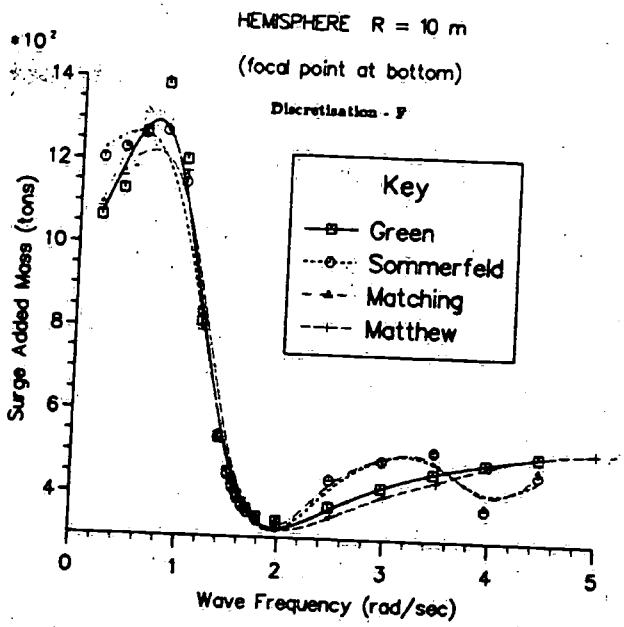

Figure 4. Discretisation F Surge Added Mass Predictions.

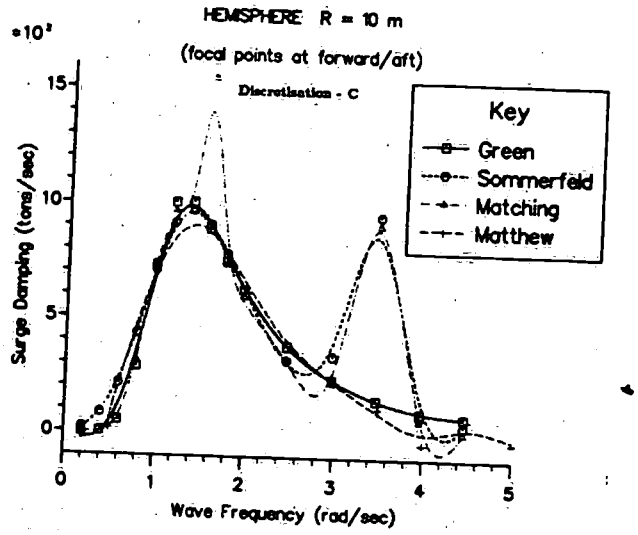

Figure 5. Discretisation C Surge Fluid Damping Predictions.

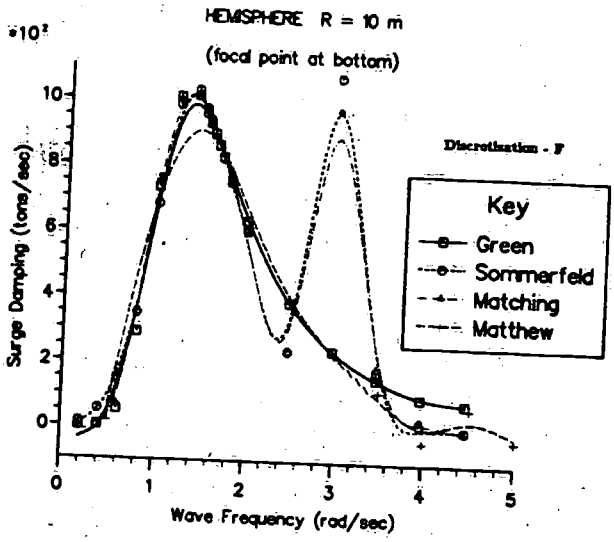

Figure 6. Discretisation F Surge Fluid Damping Predictions.

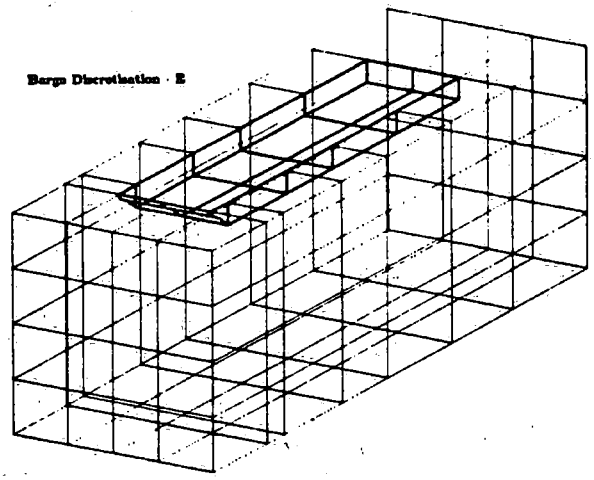

Figure 7. Barge Discretisation E.

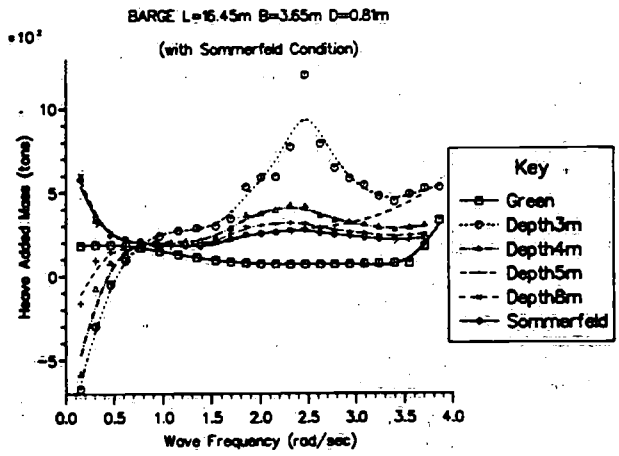

Figure 8. Heave Added Mass for Sommerfeld Matching Technique.

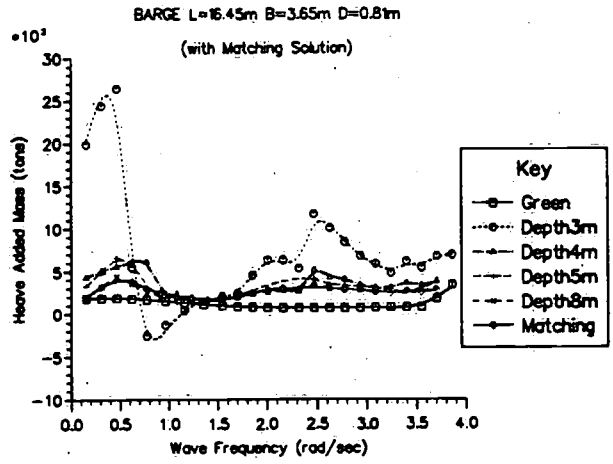

Figure 9. Heave Added Mass for HOBE GFM Technique.

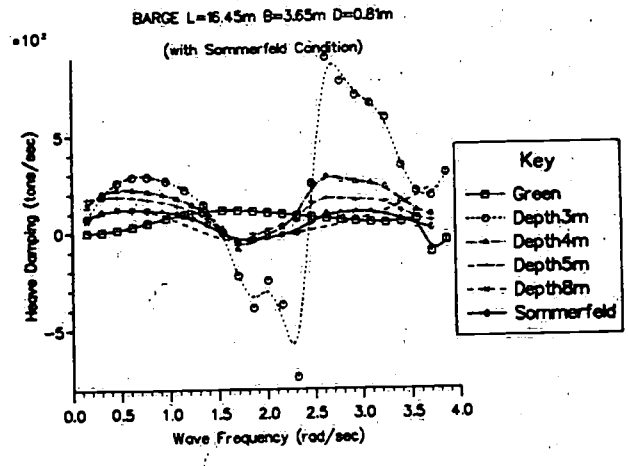

Figure 10. Heave Fluid Damping for Sommerfeld Matching Technique.

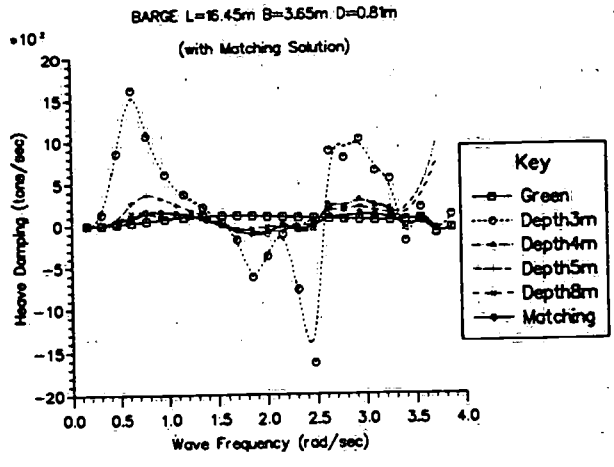

Figure 11. Heave Fluid Damping for HOBE GFM Technique.